Journal of Experimental Marine Biology and Ecology 424–425 (2012) 53–58

Contents lists available at SciVerse ScienceDirect

Journal of Experimental Marine Biology and Ecology

journal homepage: www.elsevier.com/locate/jembe

# Calcification acidifies the microenvironment of a benthic foraminifer (*Ammonia* sp.)

Martin S. Glas [a,*], Gerald Langer [b,c], Nina Keul [c]

[a] Max Planck Institute for Marine Microbiology, Celsiusstr. 1, D-28359 Bremen, Germany
[b] Department of Earth Sciences, Cambridge University, Cambridge CB2 3EQ, United Kingdom
[c] Alfred Wegener Institute for Polar and Marine Research, Am Handelshafen 12, D-27570 Bremerhaven, Germany

ARTICLE INFO

*Article history:*
Received 12 January 2012
Received in revised form 3 May 2012
Accepted 7 May 2012
Available online xxxx

*Keywords:*
Biomineralization
Calcite
Calcium
Microsensor
pH

ABSTRACT

Calcareous foraminifera are well known for their $CaCO_3$ shells. Yet, $CaCO_3$ precipitation acidifies the calcifying fluid. Calcification without pH regulation would therefore rapidly create a negative feedback for $CaCO_3$ precipitation. In unicellular organisms, like foraminifera, an effective mechanism to counteract this acidification could be the externalization of $H^+$ from the site of calcification. In this study we show that a benthic symbiont-free foraminifer *Ammonia* sp. actively decreases pH within its extracellular microenvironment only while precipitating calcite. During chamber formation events the strongest pH decreases occurred in the vicinity of a newly forming chamber (range of gradient ~100 μm) with a recorded minimum of 6.31 (<10 μm from the shell) and a maximum duration of 7 h. The acidification was actively regulated by the foraminifera and correlated with shell diameters, indicating that the amount of protons removed during calcification is directly related to the volume of calcite precipitated. The here presented findings imply that $H^+$ expulsion as a result of calcification may be a wider strategy for maintaining pH homeostasis in unicellular calcifying organisms.



## 1. Introduction

Foraminifera are abundant marine calcifiers found in virtually all marine habitats. There are approximately 10,000 extant species (Vickerman, 1992) and calcareous wall structures radiated in the Paleozoic (Ross and Ross, 1991; Tappan and Loeblich, 1988) making their calcium carbonate shells important index fossils. Together with coccolithophores, foraminifera are the major pelagic producers of calcium carbonate (Baumann et al., 2004). Their fossilization, abundance and global distribution moreover make calcareous foraminifera an important model organism for paleoceanographic reconstructions. The (trace) element and stable isotope compositions of their calcite shells are used as proxies to estimate past seawater parameters, such as temperature (Lea, 2003), salinity (Rohling, 2000), pH (Spero et al., 1997; Spivack et al., 1993) and nutrients (Elderfield and Rickaby, 2000; Rickaby and Elderfield, 1999). A process-based understanding of foraminiferal calcification is therefore essential to better interpret proxy signals.

Foraminifera grow in discrete steps of new chamber additions. Calcite precipitation in benthic rotalid foraminifera is believed to proceed in a confined space termed delimited biomineralization space (DBS). This space is actively created by the rhizopodial network around the newly forming chamber during chamber formation events (Fig. 1, model based on Erez, 2003). $CaCO_3$ precipitation is catalyzed on the surface of an organic template termed primary organic sheet (POS), being formed after establishment of the DBS (reviewed in Erez, 2003; Goldstein, 1999). In benthic rotalid foraminifera calcite wall thickening proceeds in two layers, termed 'primary calcite' on the POS of the newly forming chamber and a secondary layer termed 'secondary calcite' ((Angell, 1967), reviewed in Erez, 2003; Hansen, 1999). This secondary calcite is excreted over the complete shell surface of the foraminifera during chamber formation, resulting in a fine lamination of older chambers (Hansen, 1999).

Central to calcite precipitation by foraminifera (as in all calcifiers) is a strict control over the carbonate chemistry of the calcifying fluid. To promote $CaCO_3$ precipitation, super-saturation of the calcifying fluid needs to be maintained throughout the calcifying period. In addition, to form the delicate structures of foraminiferal shells, strict control of the timing, rate and geometry of precipitation as well as the degree of super-saturation is required (Nielsen, 1964).

It is well established that calcite precipitation strongly decreases the pH of the calcifying fluid (Zeebe and Wolf-Gladrow, 2001). Thus, biological regulated calcification, taking place in confined compartments (as in foraminifera), would rapidly shift the carbonate system towards a lower calcite saturation state without active pH compensation and thereby create a negative feedback for calcite precipitation.

We hypothesize that during chamber formation the degree of $CaCO_3$ super-saturation is controlled by active export of protons from the calcifying fluid. This excess acidification does not appear inside the cell as intracellular pH is highly regulated (reviewed in Alberts et al., 2002; Madshus, 1988). Therefore, the protons must either be neutralized or externalized. The latter mechanism implies that the proton discharge should result in an acidification of the microenvironment around the newly forming calcite.

* Corresponding author. Tel.: +49 421 2028 838; fax: +49 421 2028 690.
*E-mail address:* mglas@mpi-bremen.de (M.S. Glas).

0022-0981/$ – see front matter © 2012 Elsevier B.V. All rights reserved.
doi:10.1016/j.jembe.2012.05.006

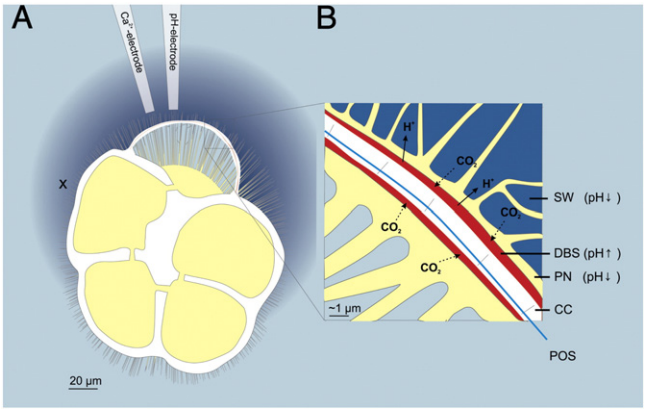


**Fig. 1.** A) Measurement settings for combined pH and $Ca^{2+}$ measurements of *Ammonia* sp. during chamber formation. Area affected by low pH gradient (idealized shape) is colored in dark blue (thickness reduced to ~1/3 for clarity). Spikes indicate the fine pseudopodial network (PN = yellow) established during chamber formation and forming the delimited biomineralization space (DBS = red). B) Close up of calcifying fluid and DBS. Increased pH within the DBS and calcification (reduction of DIC) would strongly enhance the molecular diffusion of $CO_2$ into the DBS from both the cytosol and the surrounding seawater (SW). POS = primary organic sheet (light blue), CC = $CaCO_3$ (calcite), dashed arrows indicate molecular diffusion, solid arrows indicate the active transport of ions.

We tested this hypothesis by measuring pH and $Ca^{2+}$ dynamics within the microenvironment of calcifying and non-calcifying foraminiferal specimens at different life stages with microsensors. To exclude the effect of photosynthesis, which is known to influence pH microenvironments (Rink et al., 1998), we conducted our experiments with specimens of the benthic, symbiont-free, non-phototrophic genus *Ammonia* (Cushman, 1926).

## 2. Materials and methods

### 2.1. Sampling and culturing

Specimens of a single morphotype of *Ammonia* were collected from North Sea tidal flats near Dorum, Germany (53°40′28″N 8°30′57″E) between August 2009 and June 2010. Sediments were sieved (mesh size 630 µm) to remove larger meiofauna and stored in seawater at 10 °C in the dark. Prior to experiments, adult individuals were isolated from the sediment by additional sieving through a 230 µm mesh. Reproduction was stimulated by cultivating these individuals at 25 °C and reduced salinity (to about 26) and by feeding them with sterile, heat-treated (photosynthetically inactive) microalgae of the species *Dunaliella salina*. Within 7 days about 10% of the adults reproduced asexually, yielding approximately 50–200 single-chambered juveniles (Ø ~ 50 µm) per event, which were used for the experiments.

### 2.2. Experimental setup

Microsensor measurements were performed in a large Petri dish under a backlit microscope (ZeissAxiovert 200 M) equipped with a camera (AxioCamMRc5). The Petri dish was filled with natural seawater of reduced salinity (to about 26) and contained >30 individuals. The friction velocity at the bottom of the Petri dish was adjusted to 0.2 cm $s^{-1}$ by measuring particle movement over the bottom and directing an air jet onto the water surface, to emulate natural flow conditions of tidal flat sediment surfaces (Huettel and Gust, 1992; Shimeta et al., 2001). Temperature and pH (total scale) in the bulk seawater were measured using a micro-thermometer and a handheld pH meter (WTW pH 330i), respectively.

pH LIX (precision 0.005), $Ca^{2+}$ LIX (precision 5 µM), and glass pH microelectrodes (precision 0.001) were prepared, calibrated and used as previously described (Ammann et al., 1987; De Beer, 2000; De Beer et al., 2000; Revsbech and Jorgensen, 1986). A detailed description of the measurement setup can be found in Polerecky et al. (2007). Microsensors had a tip diameter of <20 µm and were positioned around foraminifera using a robotic arm (Eppendorf PatchManNP2 system) with a precision of 50 nm.

### 2.3. Experimental procedure

Microscale measurements of pH and $Ca^{2+}$ were performed in close vicinity (<10 µm) around foraminifera and away from the calcite shell in the bulk seawater between and during chamber formation events (Fig. 2). $Ca^{2+}$ measurements were done simultaneously with pH measurements, with sensor tips separated by ~10 µm (Fig. 1A). All time series recordings of pH and $Ca^{2+}$ stated in Figs. 3, 4 and 5 were performed within the rhizopodial network for >30 min on top of the POS (<10 µm distance) as illustrated by Fig. 1A. Chamber formation was visually detected by observing pseudopodial retraction and gathering of food particles around the shell and space where the new chamber was going to be formed (reviewed in Goldstein, 1999). Throughout chamber formation, individuals remained in a fixed position attached to the bottom of the Petri dish, allowing accurate placement of the microsensor tips and ensuring a stable position of the electrode during chamber formation. The dimensions of the specimen and of the newly forming chambers were measured from the acquired time series images (software Zeiss, AxioVision 4.8.1).

### 2.4. Mass balance calculations

Calcification rates [µg $h^{-1}$] were estimated from the amount of precipitated calcite and duration of the individual chamber formation events that could be recorded completely ($n = 19$). The amount of calcite was calculated by assuming the newly formed chamber as 2/3 of an ellipsoid with radii derived from measured chamber dimensions, wall thickness of 3 µm (de Nooijer et al., 2009b) and tabulated calcite densities (DeFoe and Compton, 1925).

### 2.5. Data analyses

Linear regressions between specimen diameter (measured as largest possible diameter of individuals) and pH decreases, duration of pH decreases were assessed using Pearson product–moment correlation coefficient (R) and a general linear regression model. Regressions and statistical analyses were performed with the statistical analyses software SigmaPlot 10.0 (Systat Inc., USA).

## 3. Results

### 3.1. Microsensor measurements

During chamber formation strong pH decreases were detected near the primary organic sheet (POS) of newly calcifying chambers and in its vicinity (as illustrated by Fig. 1A) in all specimens (Fig. 2). The strongest pH decreases originated from the newly forming chambers but also extended to the neighboring chambers (Fig. 1A, indicated as point X). The difference between the maximum pH decreases recorded at the surface of the POS (Fig. 1A) and that of the surrounding seawater, denoted as ΔpH, was positively linearly correlated with the diameter of the individuals and ranged from −0.060 to −1.774 (Fig. 3). The pH decreases only occurred when chamber formation had progressed beyond the initial stage of rhizopodial network formation (~1 h) and construction of the primary organic sheet (POS; 1–3 h; Fig. 4). The onset of calcite precipitation could not be timed accurately (>3 min accuracy) by light microscopy, but was associated with an instant decrease in extracellular pH (<1 min precision, Fig. 4). The acidification persisted while the formation of pores within the calcite wall became apparent about 1–2 h

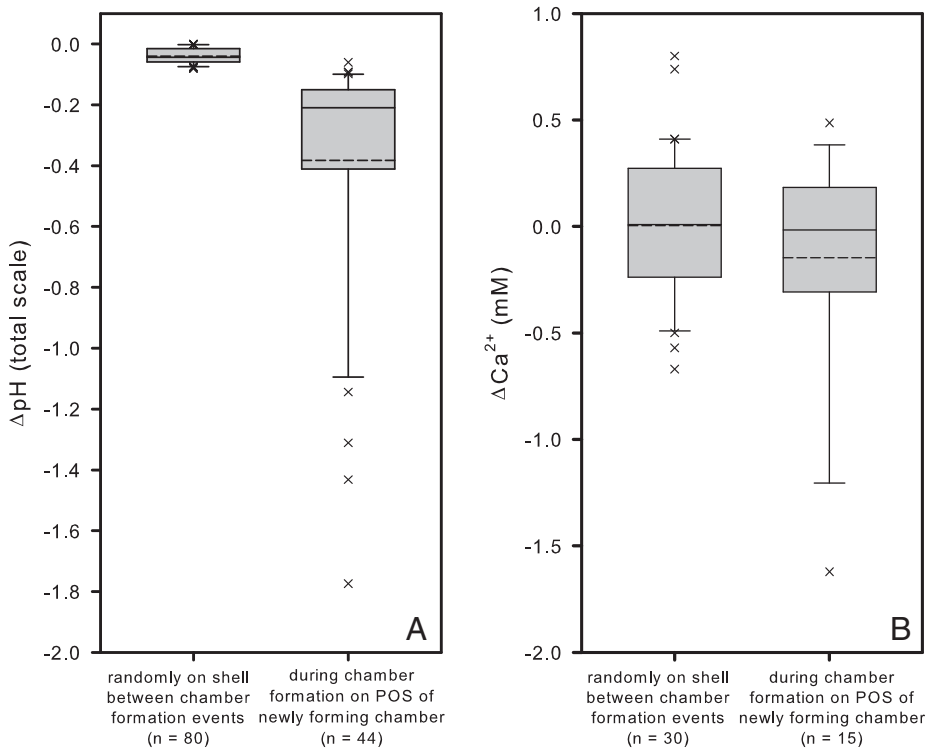


**Fig. 2.** Differences between A) pH- and B) $Ca^{2+}$-decreases and the bulk seawater (denoted as ΔpH and $\Delta Ca^{2+}$) recorded around (<10 μm from the shell) replicated ($n$) foraminiferal specimens between and during chamber formation events. Box plots show the 25th, 50th and 75th percentiles (horizontal bars). Error bars indicate the 90th and 10th percentiles. Means are indicated as dotted lines.

after the onset of calcification. The end of the chamber formation process was reached when foraminifera extended their pseudopodia and resumed movement. Shortly before and sometimes during the extension of larger rhizopodia the pH microenvironment around the foraminifera reverted back to seawater levels (Fig. 4). The timing of pH acidification of the foraminiferal microenvironment therefore exactly matched with visual signs of calcite precipitation (Fig. 4). Complete chamber formation events could be recorded in 19 cases and acidification lasted between 1 h 10 min and 7 h (Fig. 5). Durations also exhibited a positive linear correlation with the diameter of the individuals (Fig. 5). Thickness and form of the pH gradients measured from the POS surface and extending into the surrounding seawater (i.e. the 'diffusive boundary layers' = DBLs) were highly variable (50–500 μm) and strongly depended on the orientation of the new chamber in respect to flow direction and gathering of food particles, which hampered and distorted linear diffusion (data not shown). Calcification rates derived from mass balance calculations ($n = 19$) were $0.028 \pm 0.002$ (SE) μg $h^{-1}$ and ranged from 0.015 to 0.045 μg $h^{-1}$.

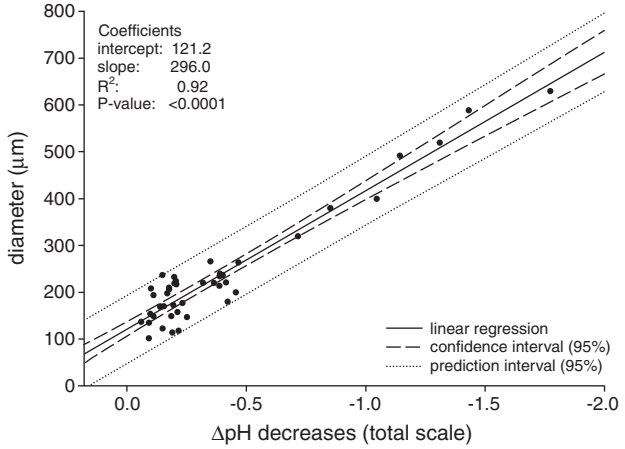


**Fig. 3.** Relationship between foraminiferal diameter and decreases of pH during chamber formation events and their linear regression ($n = 44$).

During periods between two chamber formation events only small pH variations (0 to −0.08) were detectable ($-0.040 \pm 0.003$ (mean ± SE)). These small pH decreases were not localized specifically to the surface of the shell, but recorded on all plasma membranes including rhizopodia (Fig. 2).

The established proton flux was highly regulated by the foraminifera as disturbance of the POS by gently nudging the microsensors resulted in an instant pH increase (Fig. 4), thus interrupting $H^+$ pumping. A complete breakdown of $H^+$ pumping was observed if disturbances persisted or occurred near the end of the chamber formation process. Small oscillations in pH were present in about 1/3 of all chamber formation events and persisted throughout lowered pH conditions (Fig. 4).

$\Delta Ca^{2+}$ measured on top of the POS was variable between ($4 \pm 65$ μM (mean ± SE)) and during ($-146 \pm 135$ μM (mean ± SE)) chamber formation (Fig. 2). In contrast to pH dynamics, $Ca^{2+}$ did not change significantly during chamber formation when averaged over all tested individuals compared to the surrounding seawater (paired $t$-test: $t = 1.081$, $df = 14$, $P = 0.298$, $n = 15$).

## 4. Discussion

### 4.1. Acidification due to calcification

The exact congruence of timing of the measured microenvironmental acidification with visual signs of calcite precipitation (Fig. 4), together with the fact that acidification could not be detected in periods in between two chamber formation events (Fig. 2), indicates that the pH drops are a direct consequence of localized proton removal from the site of calcification during calcite precipitation (Fig. 1B).

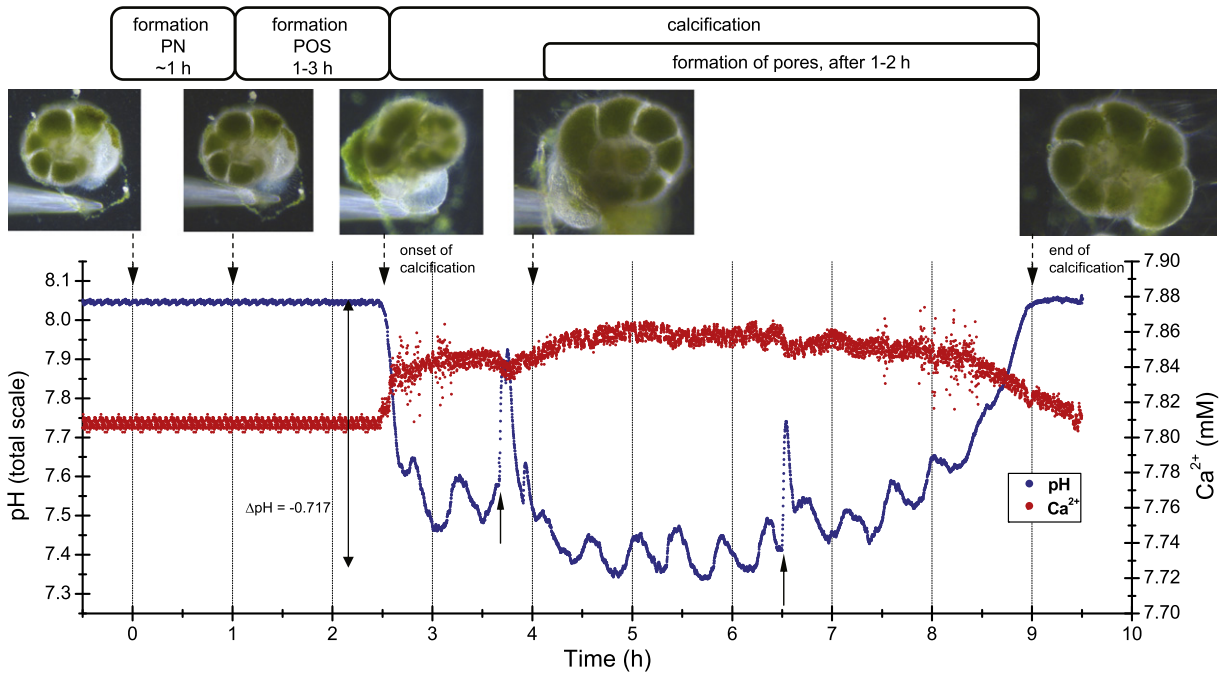


**Fig. 4.** Example of pH and $Ca^{2+}$ dynamics of an adult *Ammonia* sp. individual (diameter 320 μm) during a chamber formation event. Upward arrows indicate the moments of deliberate nudging of the POS to trigger the interruption of active proton pumping for ~5 min. Ambient water conditions: salinity 26, temperature 18 °C; incident light: 10 μmol photons $m^{-2}$ $s^{-1}$; friction velocity: 0.2 cm $s^{-1}$.

An additional indicator for this is the observed significant correlation between foraminiferal diameter and ΔpH changes (Fig. 3), following a trend of increased calcite precipitation with size. The microenvironmental acidification in the vicinity of neighboring chambers (Fig. 1A as indicated by point X) is most likely caused by secondary lamination of older chambers during chamber formation. Yet, the strongest pH drops radiated from the newly forming chamber, as a result of the high volumetric concentrations of calcite being precipitated in this region (Fig. 1A) (Hansen, 1999; Hansen and Reiss, 1971). Due to this fact, differentiating acidifications between primary and secondary layering around foraminifera was difficult.

### 4.2. Calcification rates

Calcification rates obtained by the measurements ($0.028 \pm 0.002$ (mean ± SE) μg $h^{-1}$) represent, to the best of our knowledge, the first estimates of calcification rates for *Ammonia* sp. They are lower than rates obtained by $Ca^{2+}$ labeling experiments of symbiotic planktonic foraminifera (0.04 μg $h^{-1}$ (dark) to 0.11 μg $h^{-1}$ (light) (Erez, 1983), 0.39 to 0.87 μg $h^{-1}$ (light) (Anderson and Faber, 1984), 0.06 μg $h^{-1}$ (dark) to 0.32 μg $h^{-1}$ (light) (Lea et al., 1995)). Yet, cell diameters of *Ammonia* sp. are small compared to planktonic species, suggesting decreased calcification rates with decreasing size as in coccolithophores (Langer et al., 2006; Stoll et al., 2002). Also, compared to the above labeling experiments, calcification rates determined geometrically from the formation of the ultimate chamber did not take secondary layering of the complete shell into account and thereby underestimated the amount of total calcite precipitated. Yet, calcification rates are less variable than in symbiotic foraminifera, indicating that photosynthesis is most likely the cause for increased variability of calcification rates as suggested by Lea et al. (1995).

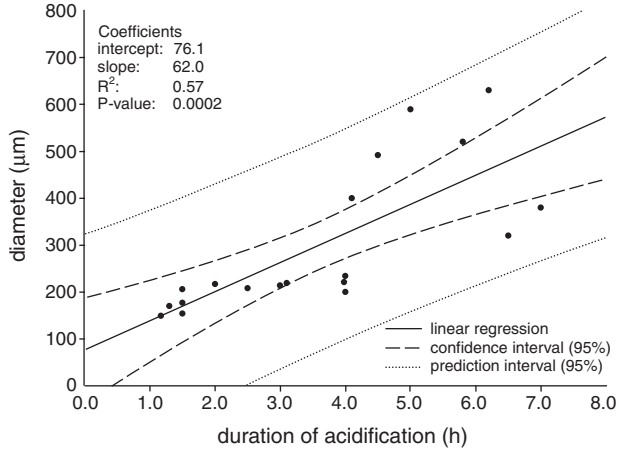


**Fig. 5.** Relationship between foraminiferal diameter and duration of pH decreases during chamber formation events that could be recorded completely and their linear regression ($n = 19$).

### 4.3. Calcium dynamics

The variability of $\Delta Ca^{2+}$ between and during chamber formation events (Fig. 2) is in accordance with previous microsensor measurements, showing high spatial variability of $Ca^{2+}$ microgradients in *Amphistegina lobifera* and *Marginopora vertebralis* (Koehler-Rink and Kuehl, 2000) and among specimens in *Orbulina universa* (Koehler-Rink and Kuehl, 2005). This indicates that $Ca^{2+}$ uptake varies temporally and spatially over the shell surface of *Ammonia* sp. (Koehler-Rink and Kuehl, 2000). The absence of an overall significant calcium gradient during chamber formation in the microenvironment can be explained in two ways: 1) $Ca^{2+}$ was not transported from the external seawater into the DBS via channel-pumping, but supplied via an intracellular calcium pool as shown by Anderson and Faber (1984), ter Kuile and Erez (1988) and ter Kuile et al. (1989). 2) $Ca^{2+}$ was transported over the complete surface of the shell (Angell, 1979). Due to the high surface area, $Ca^{2+}$ concentrations of North Sea seawater would only require a small concentration gradient to establish a high enough flux to sustain a constant rate of calcite precipitation at calcite supersaturated conditions ($\Omega_{calcite} > 1$). In both cases calcium

gradients measured within the foraminiferal microenvironment would be small, which is in accordance with the measurements.

### 4.4. Trans-membrane transport of $H^+$

We confirm that the site of calcification (i.e. the 'delimited biomineralization space') must be delineated from the bulk seawater (Angell, 1979; Be et al., 1979; Erez, 2003), as explained in the following. The microenvironment around the newly forming chamber is most likely low- or under-saturated in respect to calcite, due to the observed acidification (see also (Wolf-Gladrow and Riebesell, 1997; Wolf-Gladrow et al., 1999)). It is therefore unlikely that calcite precipitation proceeds directly from bulk seawater during chamber formation, considering the measured high calcification rates (see above). Also, if protons could diffuse freely between DBS and bulk seawater, so would other ions, e.g. $Ca^{2+}$, $Mg^{2+}$ and $Sr^{2+}$. However, measured Mg- and Sr-fractionation factors in *Ammonia* sp. cannot be explained assuming inorganic fractionation (Dissard et al., 2010), but are consistent with the hypothesis that these ions are transported across membranes before entering the calcifying fluid. It is therefore inferred that trans-membrane transport across the pseudopodial network is the means of proton removal during chamber formation (Fig. 1B). Voltage gated $H^+$-channels have recently been discovered in the protoplasma membrane of coccolithophores and are present in a wide variety of eukaryotic protists (Taylor et al., 2011).

An instant halt of trans-membrane transport of protons can also explain the pH increase in the microenvironment upon mechanical disturbance of the individual during chamber formation (Fig. 4). Another explanation could be a temporary rupture of the pseudopodial network upon mechanical disturbance and a consequent efflux of pH elevated calcifying fluid into the surrounding seawater (Fig. 1B). Yet, the acidic characteristics near the newly forming chamber were equally rapidly restored if the mechanical disturbance was not prolonged or too severe (Fig. 4). This shows that foraminifera strongly regulate calcite precipitation and/or $H^+$ removal.

After the initial drop in pH during chamber formation, pH underwent cyclic changes (Fig. 4). It can only be speculated what this pH-fluctuation might be. One possibility could be a temporary opening of the pseudopodial network around the calcifying chamber causing mixing of the high pH fluid from the DBS with the lower pH fluid of the microenvironment. The function of such a temporary opening, however, remains unclear. A replenishment of the DBS with $Ca^{2+}$ and/or dissolved inorganic carbon (DIC) cannot be the main function because such a $Ca^{2+}$-pathway would not fractionate strongly against $Mg^{2+}$ and weakly for $Sr^{2+}$ (Dissard et al., 2010), as discussed above. Another possibility could be the additional cyclic exocytosis of low pH fluid vesicles to maintain cellular pH homeostasis. Such low pH compartments have previously been identified in other benthic rotalid foraminifera during calcification (Bentov et al., 2009; de Nooijer et al., 2009a). A third explanation could be related to temporary ion transport across the plasma membrane of the pseudopodial network. Cyclic $H^+$ conductive transport pathways would hereby allow for short periods of net $H^+$-uptake and therefore extracellular temporal alkalization (reviewed in Lukacs et al., 1993).

Active $H^+$ removal from the DBS does not only result in a pH decrease in the microenvironment of a newly forming chamber, but also in a comparatively increased pH within the DBS (Fig. 1B). An advantage of such a pH increase within the DBS is related to the driving force for $CO_2$ transport. A twofold pH gradient established between the DBS, the external seawater and cytosol would strongly enhance molecular diffusion of $CO_2$ from the acidic cytosol (see also (Angell, 1979; Zeebe and Sanyal, 2002)) and external seawater into the DBS on a micro scale (0.1–5 μm distance, Fig. 1B). Such a mechanism has already been suggested for high pH seawater vacuoles during chamber formation in other species of benthic rotalid foraminifera (Bentov et al., 2009; de Nooijer et al., 2009a). Also, diffusion is the limiting factor for DIC uptake in *Amphistegina lobifera* and calcification in *Amphisorus hemprichii* (ter Kuile et al., 1989). Hence, by maintaining an increased pH to increase super-saturation with respect to calcite within the DBS, a highly efficient DIC trap would be created at the same time, facilitating bilateral diffusion of $CO_2$ into the DBS (Fig. 1B).

## 5. Conclusions

Our results show that calcification during chamber formation strongly influences the extracellular pH in the microenvironment (range of gradient ~100 μm) of the benthic foraminifer *Ammonia* sp. Additionally, within their natural habitats, i.e. tidal flat surface sediments with strongly decreased diffusivity compared with natural seawater, this pH effect is expected to be more pronounced. The here presented findings might suggest that excess $H^+$ expulsion due to calcification could be a widespread strategy for maintaining pH homeostasis in other species of calcareous rotalid foraminifera.

## Acknowledgments

We in particular wanted to thank Raphaela Schoon for the technical support with the microsensor measurements, setup and critical input to the experimental design. We also wanted to thank Gabrielle Eickert, Ines Schröder and Anja Niclas, who helped with the microsensor construction. Dirk deBeer, Jelle Bijma and the Alfred Wegener Institute in Bremerhaven are thanked for the financial support and access to the inverted backlight microscope. We are grateful to Lubos Polerecky and Dirk deBeer for their fruitful comments on the manuscript. Peter Stief is thanked for the very helpful comments on the data presentation. This research was funded by the Max Planck Institute for Marine Microbiology and the Alfred Wegener Institute through the Bioacid Projects (Martin Glas FKZ: 03F0608C, Gerald Langer FKZ: 03F0608) and the European Community's Seventh Framework Programme under grant agreement 265103 (Gerald Langer, Project MedSeA). This work contributes to EPOCA "European Project on Ocean Acidification" under grant agreement 211384. This work was funded in part by The European Research Council (ERC grant 2010-NEWLOG ADG-267931 HE). Nina Keul is the beneficiary of a doctoral grant from the AXA Research Fund. **[SS]**

## References

Alberts, B., Johnson, A., Lewis, J., Raff, M., Roberts, K., Walter, P., 2002. Molecular biology of the cell, 4th ed. Garland Science Taylor & Francis Group, New York.

Ammann, D., Bührer, T., Schefer, U., Müller, M., Simon, W., 1987. Intracellular neutral carrier based $Ca^{2+}$ microelectrode with sub-nanomolar detection limit. Pflugers Arch. 409, 223–228.

Anderson, O.R., Faber, W.W., 1984. An estimation of calcium carbonate deposition rate in a planktonic foraminifer *Globigerinoides sacculifer* using 45 Ca as a tracer; a recommended procedure for improved accuracy, pp. 303–308.

Angell, R.W., 1967. The test structure and composition of the foraminifer *Rosalina floridana**. J. Eukaryot. Microbiol. 14 (2), 299–307.

Angell, R.W., 1979. Calcification during chamber development in *Rosalina floridana*. J. Foraminifer. Res. 9 (4), 341–353.

Baumann, K.H., Böckel, B., Frenz, M., 2004. Coccolith contribution to South Atlantic carbonate sedimentation. In: Hans, R., Thierstein, J.R.Y. (Eds.), Coccolithophores: from molecular processes to global impact. Springer, Berlin, pp. 367–402.

Be, A.W.H., Hemleben, C., Anderson, O.R., Spindler, M., 1979. Chamber formation in planktonic foraminifera. Micropaleontology (New York) 25 (3), 294–307.

Bentov, S., Brownlee, C., Erez, J., 2009. The role of seawater endocytosis in the biomineralization process in calcareous foraminifera. Proc. Natl. Acad. Sci. U. S. A. 106 (51), 21500–21504.

Cushman, J.A., 1926. Recent foraminifera from Porto Rico. Publ. Carnegie Inst. Wash. 342, 73–84.

De Beer, D., 2000. Potentiometric microsensors for *in situ* measurements in aquatic environments. In: Buffle, J., Horvai, G. (Eds.), In situ monitoring of aquatic systems: chemical analysis and speciation. Wiley & Sons, London, pp. 161–194.

De Beer, D., Kuehl, M., Stambler, N., Vaki, L., 2000. A microsensor study of light enhanced $Ca^{2+}$ uptake and photosynthesis in the reef-building hermatypic coral *Favia* sp. Mar. Ecol. Prog. Ser. 194, 75–85.

de Nooijer, L.J., Toyofuku, T., Kitazato, H., 2009a. Foraminifera promote calcification by elevating their intracellular pH. Proc. Natl. Acad. Sci. U. S. A. 106 (36), 15374–15378.

de Nooijer, L.J., Langer, G., Nehrke, G., Bijma, J., 2009b. Physiological controls on seawater uptake and calcification in the benthic foraminifer *Ammonia tepida*. Biogeosciences 6 (11), 2669–2675.
DeFoe, O.K., Compton, A.H., 1925. The density of rock salt and calcite. Phys. Rev. 25 (5), 618–620.
Dissard, D., Nehrke, G., Reichart, G.J., Bijma, J., 2010. Impact of seawater pCO(2) on calcification and Mg/Ca and Sr/Ca ratios in benthic foraminifera calcite: results from culturing experiments with *Ammonia tepida*. Biogeosciences 7 (1), 81–93.
Elderfield, H., Rickaby, R.E.M., 2000. Oceanic Cd/P ratio and nutrient utilization in the glacial Southern Ocean. Nature 405 (6784), 305–310.
Erez, J., 1983. Calcification rates, photosynthesis and light in planktonic foraminifera. In: Westbroek, P., de Jong, E.W. (Eds.), Biomineralization and Biological Metal Accumulation. D. Reidel Publishing Company, Dordrecht, The Netherlands, pp. 307–312.
Erez, J., 2003. The source of ions for biomineralization in foraminifera and their implications for paleoceanographic proxies. Biomineralization 54, 115–149.
Goldstein, S.T., 1999. Foraminifera: A biological overview. In: Sen Gupta, B.K. (Ed.), Modern Foraminifera. Springer, Netherlands, pp. 37–55.
Hansen, H.J., 1999. Shell construction in modern calcareous Foraminifera. In: Sen Gupta, B.K. (Ed.), Modern Foraminifera. Springer, Netherlands, pp. 57–70.
Hansen, H.J., Reiss, Z., 1971. Electron microscopy of rotaliacean wall structures. Bull. Geol. Soc. Den. 20, 329–346.
Huettel, M., Gust, G., 1992. Impact of bioroughness on interfacial solute exchange in permeable sediments. Mar. Ecol. Prog. Ser. 89, 253–267.
Koehler-Rink, S., Kuehl, M., 2000. Microsensor studies of photosynthesis and respiration in larger symbiotic foraminifera. I The physico-chemical microenvironment of *Marginopora vertebralis*, *Amphistegina lobifera* and *Amphisorus hemprichii*. Mar. Biol. 137 (3), 473–486.
Koehler-Rink, S., Kuehl, M., 2005. The chemical microenvironment of the symbiotic planktonic foraminifer *Orbulina universa*. Mar. Biol. Res. 1 (1) ISSN 1745-1000 (print)|1745-1019(electronic).
Langer, G., Geisen, M., Baumann, K.H., Kläs, J., Riebesell, U., Thoms, S., Young, J.R., 2006. Species-specific responses of calcifying algae to changing seawater carbonate chemistry. Geochem. Geophys. Geosyst. 7 (9), Q09006.
Lea, D.W., 2003. 6.14 - Elemental and Isotopic Proxies of Past Ocean Temperatures. In: Holland, Heinrich D., Turekian, Karl K. (Eds.), Treatise on Geochemistry. Pergamon, Oxford, pp. 365–390.
Lea, D.W., Martin, P.A., Chan, D.A., Spero, H.J., 1995. Calcium uptake and calcification rate in the planktonic foraminifera *Orbulina universa*. J. Foramineferal Res. 25 (1), 14–23.
Lukacs, G.L., Kapus, A., Nanda, A., Romanek, R., Grinstein, S., 1993. Proton conductance of the plasma membrane: properties, regulation, and functional role. Am. J. Physiol. Cell Physiol. 265 (1), C3–C14.
Madshus, I.H., 1988. Regulation of intracellular pH in eukaryotic cells. Biochem. J. 250 (1), 1–8.
Nielsen, A.E., 1964. Kinetics of precipitation. Pergamon Press, Oxford.
Polerecky, L., Bachar, A., Schoon, R., Grinstein, M., Jorgensen, B.B., de Beer, D., Jonkers, H.M., 2007. Contribution of *Chloroflexus* respiration to oxygen cycling in a hypersaline microbial mat from Lake Chiprana, Spain. Environ. Microbiol. 9 (8), 2007–2024.
Revsbech, N.P., Jorgensen, B.B., 1986. Microelectrodes — their use in microbial ecology. Adv. Microb. Ecol. 9, 293–352.
Rickaby, R.E.M., Elderfield, H., 1999. Planktonic foraminiferal Cd/Ca: paleonutrients or paleotemperature? Paleoceanography 14 (3), 293–303.
Rink, S., Kuehl, M., Bijma, J., Spero, H.J., 1998. Microsensor studies of photosynthesis and respiration in the symbiotic foraminifer *Orbulina universa*. Mar. Biol. 131 (4), 583–595.
Rohling, E.J., 2000. Paleosalinity: confidence limits and future applications. Mar. Geol. 163 (1–4), 1–11.
Ross, C.A., Ross, J.R.P., 1991. Paleozoic foraminifera. Biosystems 25 (1–2), 39–51.
Shimeta, J., Starczak, V.R., Ashiru, O.M., Zimmer, C.A., 2001. Influences of benthic boundary-layer flow on feeding rates of ciliates and flagellates at the sediment-water interface. Limnol. Oceanogr. 46 (7), 1709–1719.
Spero, H.J., Bijma, J., Lea, D.W., Bemis, B.E., 1997. Effect of seawater carbonate concentration on foraminiferal carbon and oxygen isotopes. Nature 390 (6659), 497–500.
Spivack, A.J., You, C.F., Smith, H.J., 1993. Foraminiferal boron isotope ratios as a proxy for surface ocean pH over the past 21-Myr. Nature 363 (6425), 149–151.
Stoll, H.M., Klaas, C.M., Probert, I., Encinar, J.R., Alonso, J.I.G., 2002. Calcification rate and temperature effects on Sr partitioning in coccoliths of multiple species of coccolithophorids in culture. Glob. Planet. Chang. 34 (3–4), 153–171.
Tappan, H., Loeblich Jr., A.R., 1988. Foraminiferal evolution, diversification, and extinction. J. Paleontol. 62 (5), 695–714.
Taylor, A.R., Chrachri, A., Wheeler, G., Goddard, H., Brownlee, C., 2011. A voltage-gated $H^+$ channel underlying ph homeostasis in calcifying coccolithophores. PLoS Biol 9 (6), e1001085.
ter Kuile, B., Erez, J., 1988. The size and function of the internal inorganic carbon pool of the foraminifer *Amphistegina lobifera*. Mar. Biol. 99 (4), 481–487.
ter Kuile, B., Erez, J., Padan, E., 1989. Mechanisms for the uptake of inorganic carbon by two species of symbiont-bearing foraminifera. Mar. Biol. 103, 241–251.
Vickerman, K., 1992. The diversity and ecological significance of Protozoa. Biodivers. Conserv. 1 (4), 334–341.
Wolf-Gladrow, D., Riebesell, U., 1997. Diffusion and reactions in the vicinity of plankton: a refined model for inorganic carbon transport. Mar. Chem. 59 (1), 17–34.
Wolf-Gladrow, D.A., Bijma, J., Zeebe, R.E., 1999. Model simulation of the carbonate chemistry in the microenvironment of symbiont bearing foraminifera. Mar. Chem. 64 (3), 181–198.
Zeebe, R.E., Sanyal, A., 2002. Comparison of two potential strategies of planktonic foraminifera for house building: $Mg^{2+}$ or $H^+$ removal? Geochim. Cosmochim. Acta 66 (7), 1159–1169.
Zeebe, R.E., Wolf-Gladrow, D., 2001. $CO_2$ in Seawater: Equilibrium, Kinetics and Isotopes. Elsevier, Amsterdam. 346 pp.